Available online at www.sciencedirect.com

SCIENCE DIRECT

Diamond & Related Materials 14 (2005) 183–191

DIAMOND AND RELATED MATERIALS

www.elsevier.com/locate/diamond

Diamond nucleation on Ni_3Al substrate using bias enhanced nucleation method

Hou-Guang Chen*, Li Chang

Department of Materials Science and Engineering, National Chiao Tung University, Hsinchu 300, Taiwan

Received 29 March 2004; received in revised form 23 August 2004; accepted 29 October 2004
Available online 26 November 2004

Abstract

Diamond deposition with positive and negative bias enhanced nucleation (BEN) pretreatments on mirror-polished polycrystalline Ni_3Al substrates has been investigated, respectively. It was found that diamond deposition on the substrates under both biasing exhibited significant variations among grains of different orientations. The substrate surface was found to be rough in the case of negative biasing, whereas it was smooth in the case of positive biasing. Thus, the correlation of the crystallographic orientation of grains on the samples with the diamond nucleation behavior was systematically characterized for the case of positive biasing by electron backscattered diffraction method with scanning electron microscopy. Diamond deposition on Ni_3Al grains near (111) orientation results in higher nucleation densities, while the densities are low on (110) and (100) oriented grains. Also, the interfacial microstructure between diamond deposited and Ni_3Al was characterized by cross-sectional transmission electron microscopy.

Keywords: Diamond crystal; Nucleation; Chemical vapor deposition; Interface characterization

1. Introduction

Chemical vapor deposition of diamond films on various substrates has attracted intensive attention for the past decade, because it has great potentials for many important applications. However, the density of diamond nucleation on foreign substrates without any pretreatment, except for deposition on c-BN [1], is too sparse to form a continuous diamond layer that is often necessary for industrial applications. The efforts to enhance diamond nucleation on heterogeneous material substrates are important for electronic device applications. The bias enhanced nucleation (BEN) method is widely used to grow high quality diamond films on silicon and iridium substrates [2,3]. Various factors affecting diamond nucleation under the BEN process have been investigated, such as active carbonaceous species concentration, process pressure, substrate temperature, or electrical bias field, etc. [4]. In our previous study, we have shown that highly oriented diamond and high nucleation density on mirror-polished silicon substrates can be achieved easily by positive bias process, instead of conventional negative bias process [5].

In addition to the above factors, the surface orientation of substrate is also another important factor on diamond nucleation. However, few studies on the dependence of diamond nucleation on the substrate surface orientation have been carried out in the past. The orientation effect on heterogeneous nucleation has been studied in many other material systems. For example, Sukidi et al. [6] have suggested that GaP deposition on various Si oriented surfaces exhibits different incubation duration of nuclei formation. Huh et al. [7] have reported that the diamond nucleation density on the polycrystalline Ni substrate with bias enhanced nucleation pretreatment is varied from $\sim 10^4$ to $\sim 10^7$ cm^{-2} among different grains, but the relationship between the diamond nucleation density on an individual grain and the corresponding surface orientation of the grain has not been addressed.

* Corresponding author. Tel.: +886 3 5712121x55373; fax: +886 3 5724727.
E-mail address: houguang.mse88g@nctu.edu.tw (H.-G. Chen).

0925-9635/$ - see front matter © 2004 Elsevier B.V. All rights reserved.
doi:10.1016/j.diamond.2004.10.005

Table 1
Experimental parameters for diamond deposition with positive biasing

	H_2 plasma etching	BEN pretreatment	Growth
Pressure (Torr)	20	20	20
Concentration of CH_4 in H_2 (%)	0	3	1
Bias voltage (V)	No	+200	No
Duration (h)	1/4	1/4	4
Total flow rate (sccm)	300	300	300
Microwave power (W)	300	300	300
Substrate temperature (°C)	~650	750–700	700–650
Deposition apparatus	Quartz tube type MPCVD reactor with Mo disk counter-electrode		

In the present study, the polycrystalline intermetallic compound of Ni_3Al was used as the substrates for diamond deposition. Ni_3Al is Cu_3Au type structure ($L1_2$ type ordered lattice structure) with lattice constant of 3.57 Å, and may be a good candidate as the substrate for heteroepitaxial growth of diamond due to its negligible lattice mismatch with diamond (a=3.567 Å). Furthermore, Ni_3Al is usually used as the material for the aircraft turbine engine blades and other aircraft structural components because of its high melting point (1395 °C), excellent thermal stability, and good high-temperature mechanical properties [8]. As expected, we also found that the nucleation of diamond on polycrystalline Ni_3Al substrates exhibited significant variations among grains of different orientations. Electron backscattered diffraction (EBSD) with scanning electron microscopy employed to examine the relationship between the diamond nucleation density and the surface orientation as EBSD is a powerful method for the characterization of crystallographic orientation of an individual grain in small areas. We used the EBSD technique to systematically investigate the effect of the grains in different crystallographic orientations on diamond nucleation with bias enhanced pretreatment. The results will benefit for the future work of the selection of orientation of single crystal Ni_3Al for heteroepitaxial growth of diamond or other foreign material substrate for heteroepitaxial growth of diamond. Moreover, the interfacial microstructure between deposited diamond and Ni_3Al with negative and positive bias pretreatments was also characterized by cross-sectional transmission electron microscopy (XTEM).

2. Experimental procedure

The Ni_3Al ingot was prepared by the arc melting method, followed by homogenization annealing to reduce segregation and promote grain growth. The distribution of the grain size is approximately in the range from 145 μm to 1 mm, which was much larger than the resolution limit of EBSD (~0.5 μm) [9]. Before diamond deposition, each sliced specimen was polished to a mirror-like extent by Al_2O_3 suspension with 0.05 μm particle size, followed by ultrasonic cleaning in acetone for 15 min.

Diamond deposition was carried out in a stainless-steel ASTeX microwave plasma-assisted chemical vapor deposition reactor (MPCVD). Substrates were placed on a molybdenum substrate holder that was applied with negative bias field and the stainless chamber was grounded. However, in the case of positive bias enhanced nucleation, the diamond was grown by a quartz tube type MPCVD reactor. Substrates were placed on a molybdenum substrate holder at the center of the quartz tube reactor. A molybdenum disk with 30 mm diameter acted as counter-electrode was placed above the substrate, such that the substrate was positively biased. The detail configuration has been reported in previous work [5]. The substrate temperature was measured by a single-color optical pyrometer in both cases. The diamond deposition conditions with positive and negative biasing are summarized in Tables 1 and 2, respectively.

After diamond deposition, the examination of morphology and diamond nucleation density was carried out by SEM. For EBSD analysis, the EBSD pattern of each Ni_3Al grain was acquired from the regions without diamond coverage, so that the electron beam was not hindered by the diamond particles. The EBSD patterns of Ni_3Al are characteristically different from those of diamond because of the difference in crystal symmetry. Thus, it could be recognized if the beam was positioned on the Ni_3Al. The EBSD patterns were obtained from a Link Opal system attached to a JEOL JSM-6400 scanning electron microscope. XTEM was employed to characterize the interfacial structure between diamond and Ni_3Al substrate. XTEM specimens were prepared by conventional method, including grinding and polishing, followed by ion beam milling. TEM examination was performed using a Philips Tecnai 20 TEM at an acceleration voltage of 200 kV.

Table 2
Experimental parameters for diamond deposition with negative biasing

	H_2 plasma etching	BEN pretreatment	Growth
Pressure (Torr)	20	20	20
Concentration of CH_4 in H_2 (%)	0	3	1
Bias voltage (V)	No	−200	No
Duration (h)	1/4	1/3	1
Total flow rate (sccm)	300	300	300
Microwave power (W)	800	800	800
Substrate temperature (°C)	~700	750–800	850
Deposition apparatus	Stainless-steel ASTeX MPCVD reactor		

3. Results and discussion

3.1. Diamond nucleation by positive bias pretreatment

Fig. 1a shows a typical low-magnification SEM image in which diamond deposited on polycrystalline Ni_3Al substrates can be seen in significant variations among different grains with positive bias pretreatment. In higher magnification (Fig. 1b), the variation of nucleation densities over the grain boundary between Grain A and Grain D is apparently observed. Grain A has the highest diamond density, about ~ 2×10^7 cm^{-2}. The diamond density on Grains B, C, and D is ~5×10^5, ~6×10^4, and ~4×10^6 cm^{-2}, respectively. Due to the smoothness of the substrate surface, it permits us to carry out EBSD examination for orientation determination on the substrate grains with a smooth sampling surface and low defect density. The surface normal of each grain was characterized by using EBSD in SEM. The crystallographic orientations of the characterized grains are shown in Fig. 1d of a unit triangle of stereographic projection. It shows that the orientation of Grain A is located close to [111] corner, and Grains B, C and D are oriented far away from [111]. Fig. 1c is a high-magnification image showing diamond deposition on a twin in Grain C in that the strong difference in the nucleation density between the twin and the matrix of Grain C is evident as well. The diamond nucleation density on the twin is ~2×10^7 cm^{-2}. The surface normal of the twin of Grain C is also close to [111] as shown in Fig. 1d. Both Grain A and the twin of Grain C have a similar orientation and diamond density. The evidence clearly reveals the effect of surface orientation on the diamond nucleation density. On the same sample, the nucleation density varies from ~10^4 to ~10^7 cm^{-2}.

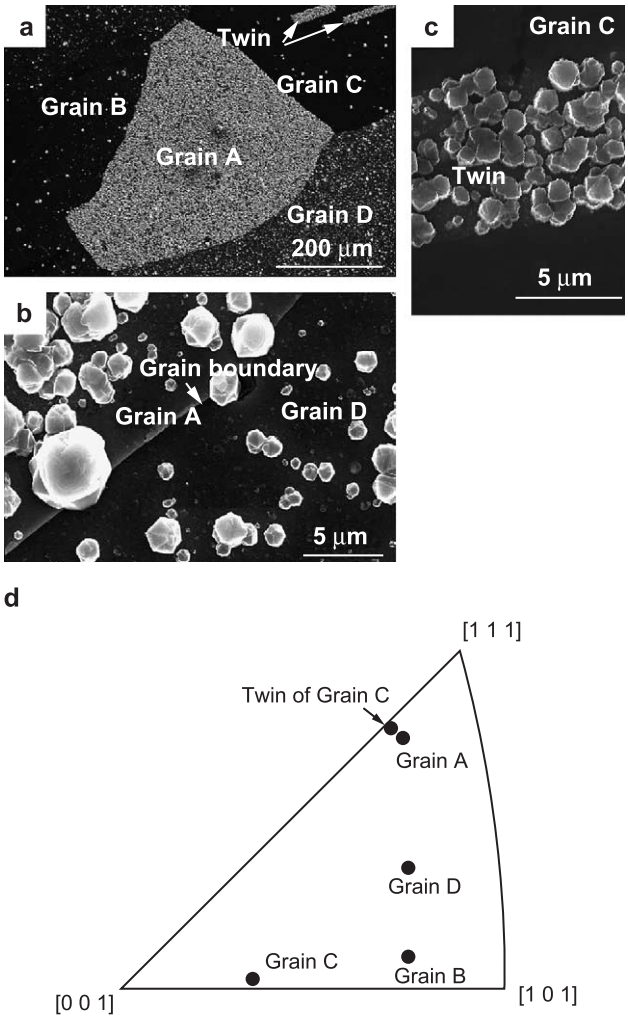

Fig. 1. (a) SEM image showing the overview of diamond deposited on Ni_3Al substrates with positive biasing. (b) High-magnification image of the region across the grain boundary between Grain A and Grain D showing the variation of nucleation densities, and (c) abrupt variations of the diamond nucleation densities between the twin and the matrix (Grain C) over the twin boundaries. (d) The unit triangle of stereographic projection shows the crystallographic orientation of each grain in (a).

Fig. 2a shows the SEM image of the diamond deposited on a grain with surface normal near Ni_3Al [111]. It is seen that no continuous film of diamond is formed. Thus, from the EBSD of uncovered region, it can be shown that the grain is misoriented from [111] zone axis with a few degrees. Since Ni_3Al is of cubic crystal system, the substrate surface is close to [111]. It appears in the SEM micrograph that the nucleation density is high in this near [111] oriented grain. The diamond deposition on a grain oriented near [110] and [100] is shown in Fig. 2b and c, respectively, revealing that the diamond particles are rarely observed. It seems that the deposition condition used in the present study results in non-oriented diamond nucleation. The reason will be examined by XTEM observation below.

The diamond deposition on several samples with wide-range orientations has been investigated using SEM with EBSD. All of the observations show the variations of diamond nucleation with Ni_3Al orientations. The results about the relationship of the diamond density with the crystallographic orientation of grains are summarized in a unit triangle of stereographic projection (Fig. 3). The unit triangle of stereographic projection can be divided into four zones according to the diamond nucleation density. The zone I, which is close to [111] corner, corresponds to the nucleation densities above ~10^7 cm^{-2}. The densities on the zone II, which is in the central region of the triangle, are in the order of ~10^6 cm^{-2}. The zone III located near [101] corner corresponds to the densities about ~10^5 cm^{-2}, and the zone IV close to [100] corner corresponds to the lowest diamond density, less than 10^5 cm^{-2}. The result indicates that positive bias pretreatment is more effectively enhanced diamond nucleation on Ni_3Al [111] face.

In our prevision study, the positive bias pretreatment was shown to enhance the diamond nucleation on Si substrates [5]. The nucleation density up to 10^9 cm^{-2} was easily achieved. During positive biasing, the negatively charged particles (such as electrons) obtain sufficient energy by the applied bias field to ionize the carbonaceous radical near the substrate surface. Therefore, the effect of enhanced diamond

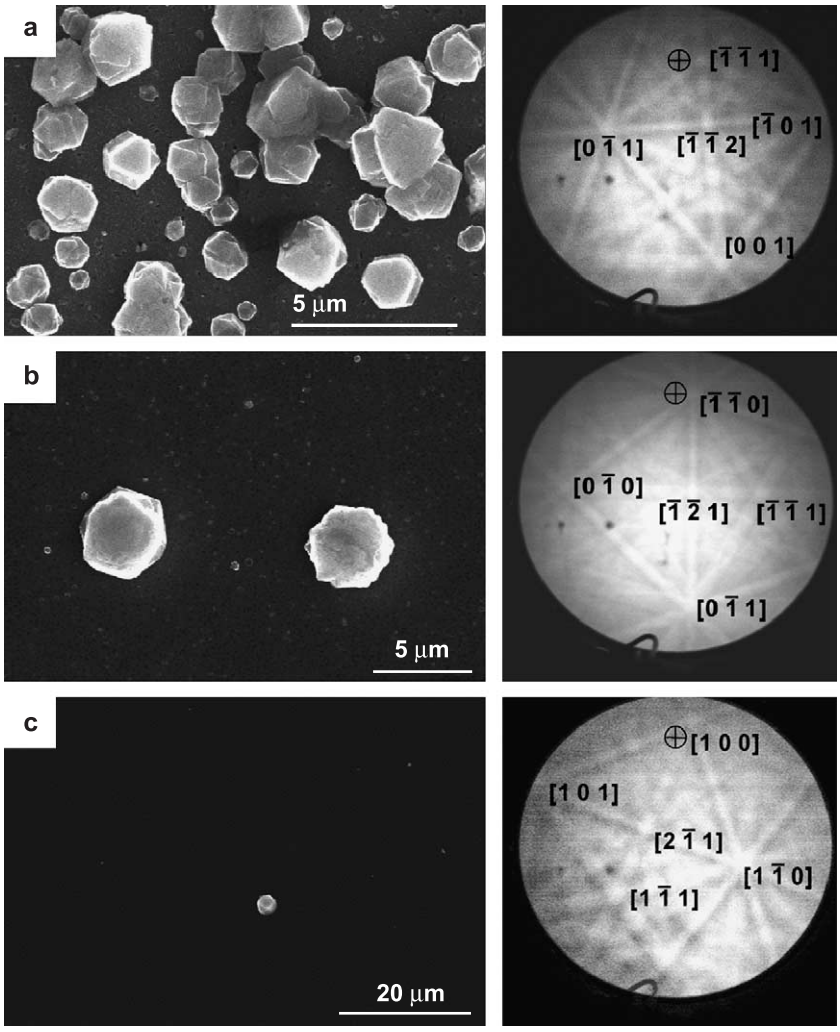

Fig. 2. SEM images of diamond deposition on surface normal (a) near Ni_3Al [111] oriented grain, (b) near [110] oriented grain, and (c) near [100] oriented grain, and the EBSD patterns of the corresponding Ni_3Al grains with surface normal (a) near [111], (b) near [110], and (c) near [100].

nucleation under positive biasing can be achieved. However, our observations reveal that the diamond density is varied from 10^4 to 10^7 cm^{-2} among Ni_3Al grains with different orientations. It is noticed that the diamond nucleation density on polycrystalline Ni_3Al without any biasing ranges from 10^4 to 10^5 cm^{-2}. It implies that the bias pretreatment on Ni_3Al is not able to enhance the diamond nucleation in certain orientations, and the variations of surface kinetics on faces of different orientation may have a much stronger effect on diamond nucleation instead, due to the crystalline anisotropy among Ni_3Al grains. Diamond nucleation on Ni_3Al exhibits the island morphology, resulting from the much higher surface energy of diamond. In such a nucleation mode, the surface migration and adsorption of carbonaceous species to form stable nuclei also governs eventually the nucleation rate. The migration and adsorption of carbonaceous radical species on foreign substrate surface depends strongly upon the surface structure and surface energy that vary closely with surface orientations. Because of ordered lattice structure of Ni_3Al, the ratio of the Ni and Al atoms on the surface is different in various orientations. In [111] face, the ratio of Ni to Al atoms is 3:1, whereas in both [110] and [100] faces it can be either 1:1 or purely Ni

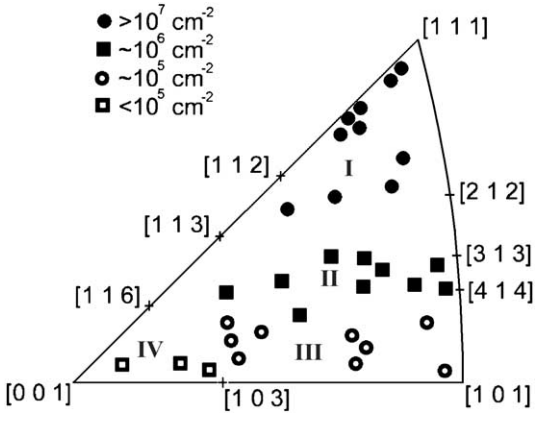

Fig. 3. The unit triangle of stereographic projection showing the orientations corresponding to various diamond nucleation densities.

atoms on these faces. From the results of Ni_3Al surface analysis, the face of the ratio 1:1 consistently exists on [110] and [100] outmost layer [10–13]. The different species of atom on Ni_3Al surface could have various degrees of affinity with carbonaceous species and atomic hydrogen, resulting in the different levels of chemical bonding with foreign species. It has been shown that Al–C bond is stronger than Ni–C bond in the study of carbon atom bonding with Al and Ni in Ni_3Al grain boundaries [14]. Thus, it is possible that Al may have more affinity with carbon than Ni, in spite of the different structure between the grain boundary and the surface. As a result, Al–C bonding could retard the surface diffusion of carbonaceous species to form diamond nuclei on Ni_3Al [110] and [100] surfaces, such that diamond nucleation is limited.

XTEM characterization of diamond nucleation on Ni_3Al with the positive bias pretreatment was also carried out. Fig. 4a shows the XTEM bright field image of the microstructure of the interface between diamond and Ni_3Al substrate. It is noticed that the interface between diamond and Ni_3Al substrate is quite smooth. Furthermore, it can be seen that an interlayer between diamond grain and Ni_3Al substrate exists, and the thickness of the interlayer is approximately 15 nm. Fig. 4b and c shows the selected area diffraction (SAD) patterns of diamond and Ni_3Al substrate, respectively. In Fig. 4b, the selection area diffraction pattern of the diamond shows twinned diamond characteristics which have streaks in the pattern and 1/3{111} forbidden reflection spots, as indicated by white arrowheads. The composition of the interlayer would be qualitatively identified by EDS, and showed that the carbon K_α characteristic peak was dominant signal with little Ni and Al signals. Hence, the interlayer might be of amorphous carbon. As the interlayer formed prior to diamond nucleation, it might preclude the oriented growth of diamond on Ni_3Al with positive bias pretreatment. However, it is hard to know if the interfacial structure on other oriented Ni_3Al grains is similar to that shown in Fig 4a, due to the difficulty of TEM specimen preparation in precision and the limited

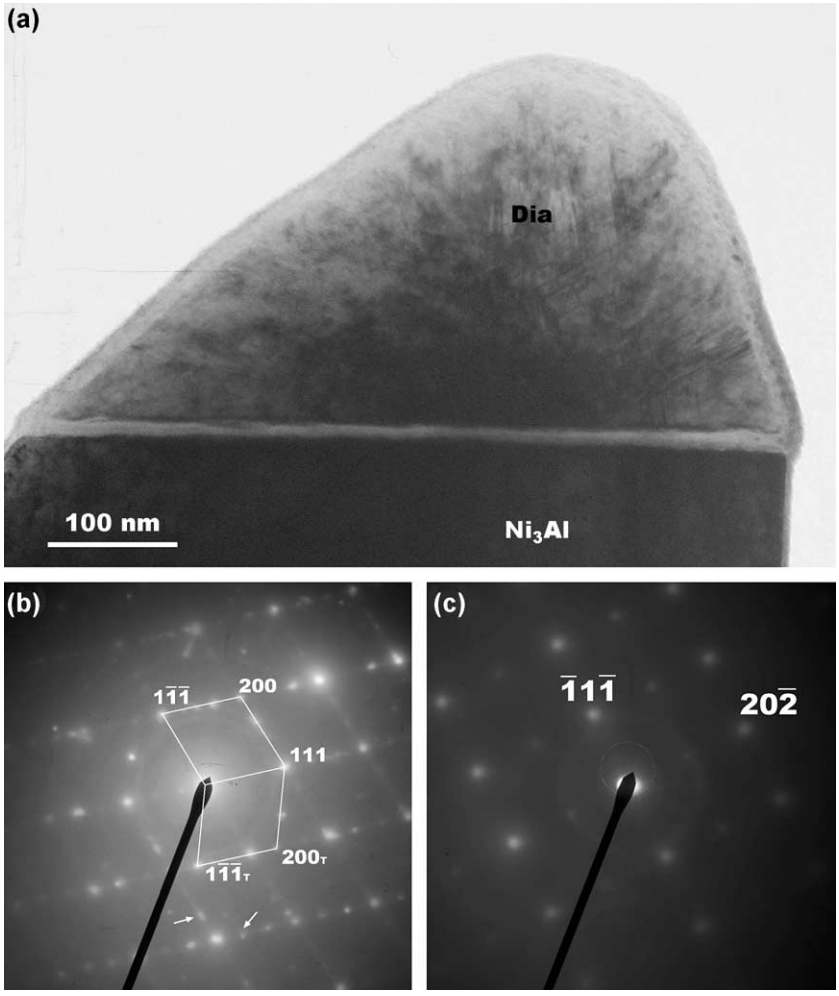

Fig. 4. (a) XTEM bright field image of diamond deposited on Ni_3Al with positive biasing. An interlayer between diamond and Ni_3Al substrate can be observed. (b) SAD pattern of twinned diamond in [01$\bar{1}$] zone axis. The white arrowhead indicate 1/3{111} forbidden reflection spots contributed from twins in diamond. (c) SAD pattern of Ni_3Al substrate in [121] zone axis.

region for TEM examination. For further TEM characterization on the interface between diamond and specific Ni_3Al grains, it will be necessary to employ focused ion beam method to prepare precision-cut cross-sectional TEM samples from the designated regions.

3.2. Diamond nucleation by negative bias pretreatment

The negative bias pretreatment in diamond deposition on polycrystalline Ni_3Al substrates also results in variations of nucleation among different grains. Fig. 5a shows a typical low-magnification SEM image. The difference in the nucleation density of diamond on the Ni_3Al grains causes the different contrast of the SEM image. The brighter contrast corresponds to higher densities of diamond. SEM images at various magnifications in Fig. 5b and c reveal the difference of diamond nucleation density on two adjacent grains. The diamond nucleation density on one of the grains is about 2×10^8 cm^{-1}, higher than 7×10^7 cm^{-1} on the other. The diamond morphology on both grains is similar as shown in Fig. 5d and e, respectively, that the diamond crystallites with {111} and {100} facets exhibit polycrystalline habits. It is noticed that there are a large number of particles and pits in nanometer scale surrounding the diamond crystallites on all the Ni_3Al grains of high and low diamond density (see Fig. 5f). Unfortunately, the relationship between the diamond nucleation density and the corresponding orientation of Ni_3Al grain cannot be obtained by EBSD method because of the rough substrate surface.

To realize the interfacial microstructure between diamond and Ni_3Al substrate, XTEM characterization was employed as well. Fig. 6a is a XTEM bright field micrograph which shows two diamond crystallites grown on Ni_3Al substrate. The SAD pattern of substrate in Fig. 6b is shown to be the typical pattern of single crystal Ni_3Al in

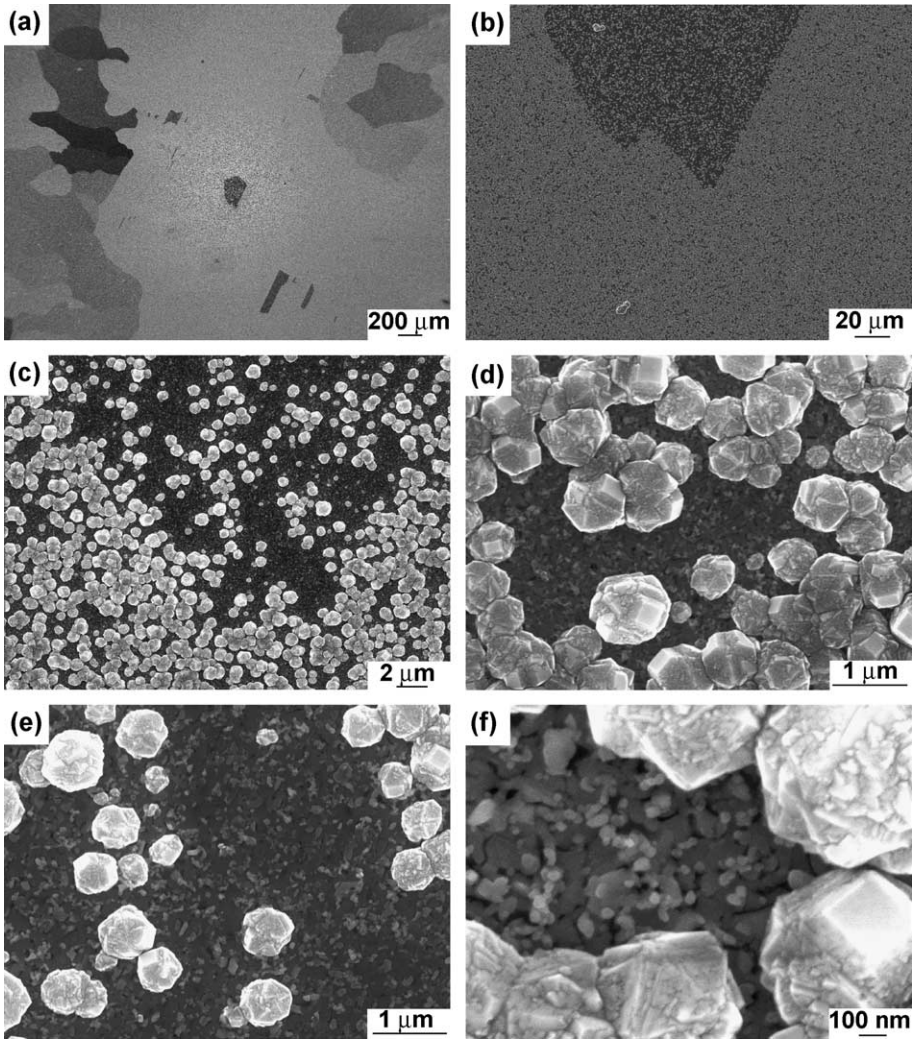

Fig. 5. (a) Low-magnification SEM image showing the overview of diamond deposited with negative bias pretreatment on Ni_3Al substrate. The brighter areas correspond to higher nucleation densities of diamond. (b) and (c) SEM images at various magnifications indicating the difference of diamond nucleation density on the two different grains. (d) High-magnification image showing diamond deposited on the grain with high nucleation density. (e) High-magnification image showing diamond deposited on the grain with low nucleation density. (f) A large number of nanometer-sized particles and pits accompanying diamond.

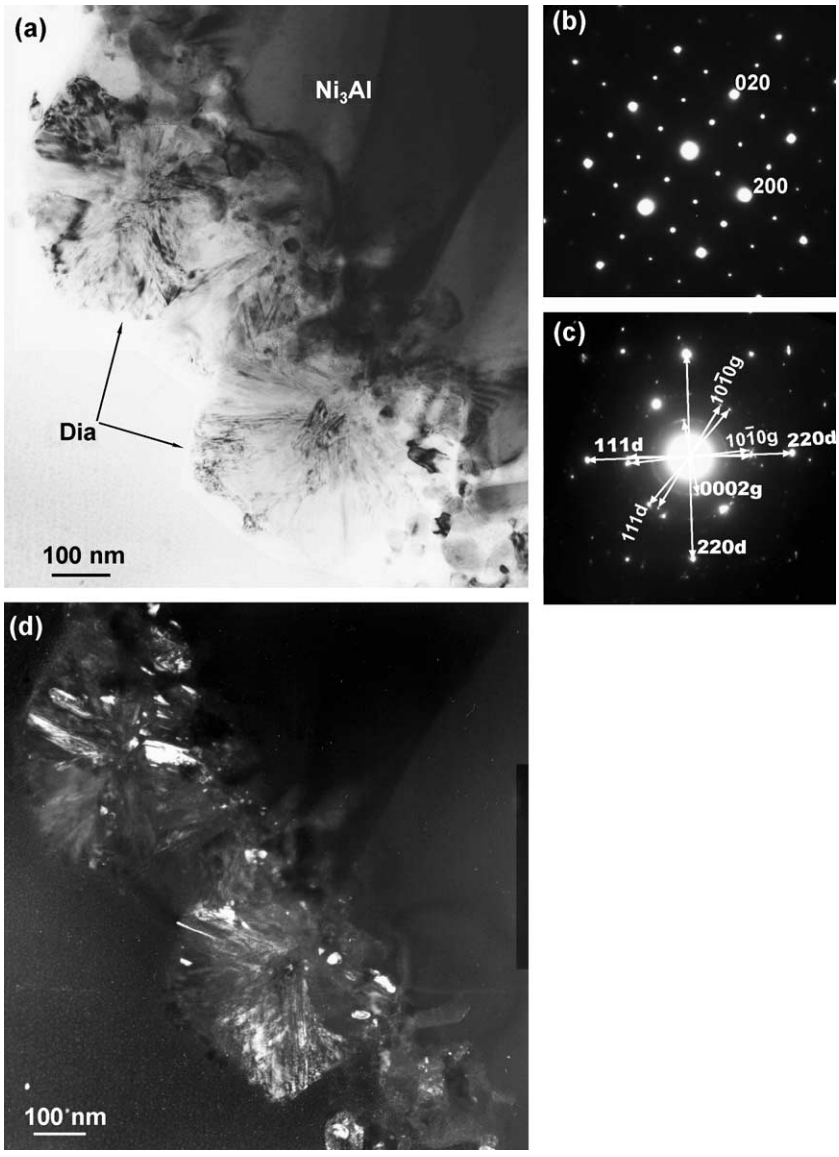

Fig. 6. (a) XTEM bright field image of diamond deposited on Ni_3Al with negative biasing. (b) SAD pattern of substrate showing typical Ni_3Al in [001] zone axis. (c) SAD pattern showing the graphite phase with diamond. (d) Dark field image showing that diamond crystallites contain many defects in twins and grain boundaries.

[001] zone axis. In contrast to Ni_3Al substrate, the SAD pattern of diamond exhibits poly-crystalline characteristics (Fig. 6c). The diamond crystallites contain many defects, such as twin and grain boundaries, as demonstrated in Fig. 6d of a dark field image. It is observed that the interface between diamond and Ni_3Al substrate is very rough. It is speculated that the intense ion bombardment during negative bias pretreatment might cause etching of the substrate. Apart from diamond, the graphite phase also can be identified from the diffraction pattern (Fig. 6c). The ring pattern in the inner side of the SAD pattern has an interplanar spacing of 0.34 nm, which corresponds to graphite 0002 reflection. The nano-particles that have previously mentioned in SEM were also found in TEM as shown in Fig. 7. The nano-particles are encapsulated in epoxy on the Ni_3Al substrate. It is noticed that the faceting of these nano-particles can be clearly observed, suggesting that these nano-particles are crystalline. In order to analyze the crystallographic structure of the nano-particles, the micro-diffraction technique was used. The top-right inset is a micro-diffraction pattern of Ni_3Al substrate and the top-left one is the pattern of the nano-particle as indicated by black arrowhead. The micro-diffraction pattern of the nano-particle exhibits a typical Ni_3Al diffraction pattern in [011] zone axis. Although the explicit cause for the formation of nano-particles is not clear yet, it is possible that it is closely related to the bombardment of charged carbonaceous radicals onto the substrate surface during negative bias pretreatment. We had applied pure hydrogen plasma to Ni_3Al substrate for 30 min under the same negative bias condition to see if there was any etching effect; however, no nano-particles could be found on the substrate surface which

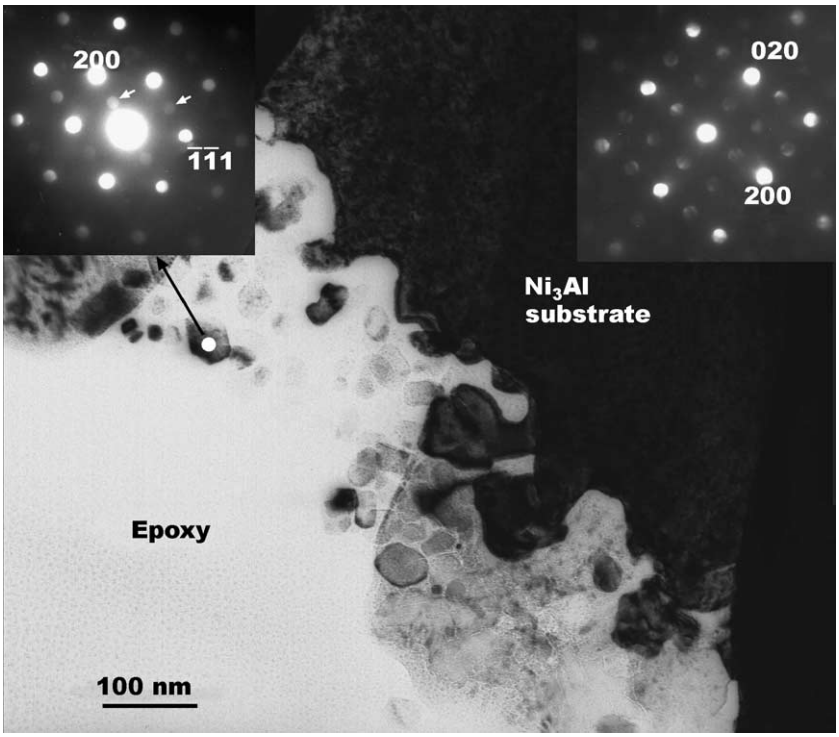

Fig. 7. XTEM image of nano-particles on Ni_3Al substrate. The top-right inset showing the micro-diffraction pattern of Ni_3Al substrate in [001] zone axis; and the top-left inset showing the micro-diffraction pattern taken from one of these nano-particles which has superlattice reflection spots (indicated by white arrowheads) in single crystalline Ni_3Al [011] zone axis.

remained to be smooth. Surprisingly, further experiment showed that the nano-particles and pits occurred immediately on the substrate surface, soon after methane addition into hydrogen during the negative bias pretreatment. Thus, the charged carbonaceous ion bombardment is probably responsible for formation of nano-particles and roughening of the substrate surface.

In XTEM observations, the interface structure in both cases of negative and positive biasing is significantly different. Similar situation was also discovered in previous study which diamond grew on $CoSi_2$ substrate with negative and positive bias pretreatments, respectively [15]. In the negative biasing case, an extremely rough interface between diamond and $CoSi_2$ was also obtained due to ion bombardment during biasing. In contrast, the smooth interface structure can be seen under positive biasing. During positive biasing, though the substrate suffers bombardments of the charged particles, which are electrons, the etching effect of bombardment is negligible due to little mass of electron.

Also, the orientation effect of Ni_3Al substrate plays an important role on diamond nucleation in the case of negative biasing. During negative biasing, the positively charged carbonaceous ions are accelerated by electric field to bombard substrate [16–18]. Ni_3Al as ordered intermetallic compound has significant variations in composition and atom packing of Ni and Al atoms in different orientations with which it exhibits highly crystallographic anisotropy. It has been shown that Al has much higher Ar ion sputter yield than Ni in the ion energy range of 0.1–4.0 keV [19]. Similar phenomenon also can be found in other ordered intermetallic compounds, for example, Cu_3Au, which has the same crystal structure as Ni_3Al [20]. Therefore, orientation-dependent sputter yield occurs. Similar situation might also happen in the present case of negative biasing which results in preferential sputtering on certain oriented grains. Consequently, the variations of sputtering might result in the heterogeneous diamond nucleation. Furthermore, the variations of the foreign carbonaceous species surface migration and adsorption on different crystallographic faces might also cause the observable heterogeneity in diamond nucleation. Interestingly, in a preliminary study of diamond deposition on poly-crystalline silicon substrate with negative biasing, we also found similar heterogeneous diamond nucleation on differently oriented grains. Nevertheless, the behavior of diamond nucleation under negative and positive biasing strongly depends on surface orientation of substrate.

4. Conclusions

Diamond deposition with positive and negative bias enhanced nucleation pretreatments, respectively, on mirror-polished polycrystalline Ni_3Al substrates with varied crystallographic orientation has been investigated. Both bias pretreatments resulted in significant variations of diamond nucleation on different Ni_3Al grains that are

orientation-dependent. According to SEM and XTEM characterization, the negative bias pretreatment results in surface roughening of Ni_3Al and forming Ni_3Al nanoparticles around the diamonds, whereas the relatively smooth and clean surface of Ni_3Al can be obtained with positive biasing. The negative bias pretreatment can enhance the diamond nucleation density up to 2×10^8 cm^{-2}. In the case of positive biasing, the relationship between the diamond nucleation density and the corresponding substrate surface orientation was systematically investigated. Positively bias-enhanced nucleation of diamond is more effective on Ni_3Al [111] face. On the Ni_3Al grains near [111] orientation, high nucleation densities of diamond $\sim10^7$ cm^{-2} can be obtained, however, diamond densities are very low on the [110] and [100] oriented grains.

Acknowledgements

This work was supported by the National Science Council, Taiwan, ROC under contract of NSC 90-2216-E-009-028. We thank Ms. Guey-Shiang Chen (Institute of Materials Science and Engineering in National Sun Yat-Sen University) for the assistance of EBSD operation.

References

[1] H. Maeda, S. Masuda, K. Kusakabe, S. Morooka, Diamond Relat. Mater. 3 (1994) 398.
[2] X. Jiang, M. Fryda, C.L. Jia, Diamond Relat. Mater. 9 (2000) 1640.
[3] M. Schreck, H. Roll, B. Stritzker, Appl. Phys. Lett. 74 (1999) 650.
[4] H. Liu, D.S. Dandy, Diamond Relat. Mater. 4 (1995) 1173.
[5] T.F. Chang, L. Chang, J. Mater. Res. 16 (2001) 3351.
[6] N. Sukidi, K.J. Bachmann, V. Narayanan, S. Mahajan, J. Electrochem. Soc. 146 (1999) 1147.
[7] J.M. Huh, D.Y. Yoon, Diamond Relat. Mater. 9 (2000) 1475.
[8] N.S. Stoloff, Int. Mater. Rev. 34 (1989) 153.
[9] K.Z. Baba-Kishi, J. Mater. Sci. 37 (2002) 1715.
[10] Y.G. Shen, D.J. O'Connor, R.J. Macdonald, Surf. Interface Anal. 18 (1992) 729.
[11] Y.G. Shen, D.J. O'Connor, R.J. Macdonald, Surf. Interface Anal. 17 (1991) 903.
[12] D. Sondericker, F. Jona, P.M. Marcus, Phys. Rev., B 33 (1986) 900.
[13] D. Sondericker, F. Jona, P.M. Marcus, Phys. Rev., B 34 (1986) 6775.
[14] I. Osamu, T. Hideki, Acta Metall. Mater. 43 (1995) 2731.
[15] M.R. Chen, L. Chang, T.F. Chang, H.G. Chen, Mater. Chem. Phys. 72 (2001) 172.
[16] X. Jiang, C.L. Jia, M. Szameitat, C. Rickers, Phys. Rev., B 64 (2001) 245413.
[17] S. Yugo, T. Kimura, T. Kanai, Diamond Relat. Mater. 2 (1993) 328.
[18] J. Gerber, S. Sattel, K. Jung, H. Ehrhard, J. Robertson, Diamond Relat. Mater. 4 (1995) 559.
[19] S. Hofmann, M.G. Stepanova, Appl. Surf. Sci. 90 (1995) 227.
[20] Th.J. Colla, H.M. Urbassek, Nucl. Instrum. Methods Phys. Res., B Beam Interact. Mater. Atoms 152 (1999) 459.